

Stress Relaxation in Entangled Polymer Melts

Carsten Svaneborg,^{1,*} Jixuan Hou,² Ralf Everaers,² and Gary S. Grest³

¹*Department of Chemistry and Interdisciplinary Nanoscience Center (iNANO),
University of Aarhus, Langelandsgade 140, DK-8000 Aarhus C, Denmark*

²*Laboratoire de Physique and Centre Blaise Pascal of the École
Normale Supérieure de Lyon, Université de Lyon, CNRS UMR 5672,
46, allée d'Italie, 69364 Lyon cedex 07, France*

³*Sandia National Laboratories, Albuquerque, NM 87185, USA*

We present an extensive set of simulation results for the stress relaxation in equilibrium and step-strained bead-spring polymer melts. The data allow us to explore the chain dynamics and the shear relaxation modulus, $G(t)$, into the plateau regime for chains with $Z = 40$ entanglements and into the terminal relaxation regime for $Z = 10$. Combined with the known (Rouse) mobility of unentangled chains and the results of the primitive path analysis of the microscopic topological state, we have performed parameter-free tests of several different tube models.

PACS numbers: 83.80.Sg (Polymer melts), 83.10.Rs (MD simulation rheology), 61.25.he (liquid structure polymer melt)

High molecular weight polymeric liquids display remarkable viscoelastic properties [1, 2]. Contrary to glassy systems, their macroscopic relaxation times are not due to slow dynamics on the monomer scale, but arise from the chain connectivity and the restriction that the backbones of polymer chains cannot cross while undergoing Brownian motion. Modern theories of polymer dynamics [3, 4] describe the universal aspects of the viscoelastic behavior based on the idea that molecular entanglements confine individual polymers to tube-like regions in space. Nearly forty years after the initial conception [5, 6], the development of a quantitative, microscopic theory remains a challenge. Validation of the complex relaxation scenario based on a combination of local Rouse dynamics, reptation, contour length fluctuations, and constraint release [4] crucially depends on the availability of experimental and simulation data for model systems.

Entangled polymers are studied experimentally using rheology [1, 2, 7], dielectric spectroscopy [8], small-angle neutron scattering [9, 10], and nuclear magnetic resonance [11, 12]. Computer simulations [13–16] offer some advantages in the preparation of well-defined model systems and the simultaneous access to macroscopic behavior and microscopic structure and dynamics. In particular, the recently developed primitive path analysis (PPA) [17–24] reveals the experimentally inaccessible *mesoscopic* structures and relaxation processes described by the tube model and allows *parameter-free* comparisons between theoretical predictions and data. However, the long relaxation times pose a particular challenge to computational techniques. Here we present simulation results for model polymer melts in equilibrium and after a rapid, volume-conserving uni-axial elongation. We have been able to follow the full relaxation dynamics deep into the entangled regime and present the first parameter-free test of the predictions of tube models for dynamical properties.

Our numerical results are based on extensive molecular dynamics (MD) simulations of bead-spring polymer melts [13]. Each chain is represented as a sequence of beads connected by finite-extensible, non-linear elastic (FENE) springs, while excluded volume interactions are described by the repulsive part of the Lennard-Jones 12-6 potential (LJ). The energy scale is set by the strength of the LJ interaction, ϵ , while the distance scale is set by the monomer size, σ . The basic unit of time is $\tau = \sigma(m/\epsilon)^{1/2}$, where m is the mass of each monomer. The equations of motion are integrated using the LAMMPS MD simulation package [25] with a velocity Verlet algorithm and a time step $\delta t = 0.012\tau$. The temperature, $T = \epsilon/k_B$, was kept constant by weakly coupling the motion of each bead to a heat bath with a local friction $\Gamma = 0.5\tau^{-1}$.

We have studied seven entangled polymer melts of M chains of N beads with $M \times N = 5000 \times 50, 2500 \times 100, 400 \times 175, 200 \times 350, 200 \times 700, 400 \times 1000$, and 320×3500 each at a monomer density $\rho = 0.85\sigma^{-3}$. Using the most refined PPA estimate of the rheological entanglement length for this model of $N_e = 90 \pm 10$ [24], the investigated system span the range from unentangled ($Z = N/N_e \approx 0.5$) to highly entangled ($Z = N/N_e \approx 39$). The Rouse time was previously determined as $\tau_R = 1.5\tau N^2$ [13], entanglements effects become relevant around $\tau_e = \tau_R(N_e)$, and the maximal relaxation times of entangled systems are expected to be on the order of $\tau_d^0 = \tau_e Z^3 = \tau_R Z$.

The melts were generated and equilibrated following the procedure outlined in Auhl *et al.* [16]. Technically, the largest challenge is the reliable extraction of the macroscopic, viscoelastic behavior [26, 27]. Data were recorded in equilibrium as well as out of equilibrium after a step-strain. Strained melts were prepared by subjecting equilibrated initial conformations to rapid ($T_{def} \in [120\tau, 36000\tau]$), volume-conserving ($\lambda_x \lambda_y \lambda_z \equiv 1$), elongational deformations with ($\lambda_x = \lambda, \lambda_y = \lambda_z = 1/\sqrt{\lambda}$) for

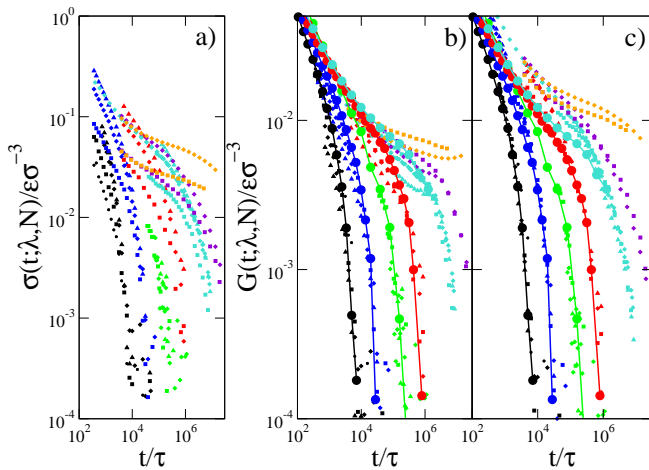


FIG. 1: (color online) (a) Relaxation of the normal stress in strained model systems. (b) Shear moduli obtained from Doi-Edwards damping function and (c) the Rubinstein-Panyukov slip-tube model. Data for step-strained melts $N = 50, 100, 175, 350, 700, 1000,$ and 3500 (curves left to right) and strain $\lambda = 1.5$ (\star), 2 (\square), 3 (\diamond), and 4 (\triangle). Relaxation moduli obtained from the Green-Kubo relation (solid \circ , solid line). Data for $N = 50, 100,$ and 350 from Ref. [27]. Data for $N = 175$ and 700 , this work.

λ ranging from 1.5 to 4.0. In the ideal case, strain should be introduced instantaneously. To check the dependence of our results on T_{def} , we have varied the deformation time in one case ($N = 700, \lambda = 3.0$) by a factor of 200. In the following, for deformed systems, $t = 0$ is fixed to the *middle* of the deformation period, i.e. data are recorded for $t \geq T_{def}/2$. To reduce finite- T_{def} artifacts, we typically discard data from the initial $3T_{def}$.

The longest simulations were run up to 2×10^9 time steps and sufficient to completely relax all but the longest chain systems ($2 \times 10^9 \times 0.012\tau = \tau_R(N = 4000) = \tau_d(Z = 12.5)$). The total numerical effort corresponds to about 5 million single core CPU hours. We recorded block-averages of the microscopic stress tensor $\sigma_{\alpha\beta}(t) = \langle \sum_{ij} F_{ij,\alpha} r_{ij,\beta} \rangle / V$ at intervals of 1.2τ . The latter sum is over all pairs i, j of interacting beads, α, β are Cartesian indices, and F, r and V denotes force, separation and volume, respectively. Furthermore, we stored melt conformations at intervals of 120τ for further analysis of the chain conformations.

Results for the relaxation of the normal tension $\sigma(t) = \sigma_{xx} - \frac{1}{2}(\sigma_{yy} + \sigma_{zz})$ are presented in Fig. 1a. We observe a clear non-Newtonian behavior with a stress relaxation extending over many orders of magnitude in time after the end of the deformation period of the sample. As expected, there is a strong increase of the terminal relaxation time with chain length and the gradual formation of an intermediate plateau in the stress relaxation for the longest chains studied. The maximal relaxation time is independent of the total deformation.

We are mainly interested in the shear relaxation modulus $G(t) = \sigma_T(t; \lambda)/h(\lambda)$. Our systems are too small, to generate a measurable elastic response in the linear regime of deformations of the order of a few percent. As in the case of the shear modulus of polymer networks [26] we extract $G(t)$ by dividing the measured normal tensions by a suitable damping function $h(\lambda)$. Dampening functions account for fast relaxation processes and for the non-linearity of the elastic response, while the shear relaxation modulus describes the slow relaxation of the deformed tube structure [3, 28, 29]. This stress-time separability is experimentally well established for melts of long relatively monodisperse chains [30].

There are a number of models for the dampening function $h(\lambda)$. Classical rubber elasticity assumes that the deformation of the melt structure is affine on all length scales in which case $h(\lambda) = \lambda^2 - \lambda^{-1}$. The Rubinstein-Panyukov slip-tube model [31] describes the stress-strain behavior of polymer networks as the sum of a crosslink and an entanglement contribution. We have previously shown that this model works very well for crosslinked networks. [32] The entanglement contribution takes chain length redistribution inside the tube into account and predicts for melts of long chains

$$h(\lambda) = \frac{\lambda^2 - \lambda^{-1}}{0.74\lambda + 0.61\lambda^{-1/2} - 0.35} \quad (1)$$

Doi and Edwards [33] derived a more complex expression retaining the assumption of affine deformation, but including the effects of a uniform chain retraction inside the tube.

Figures 1bc shows a comparison between the relaxation moduli we obtained from our step-strained melts using the two different dampening functions, and relaxation moduli obtained by Likhtman *et al.* [27] and ourselves via the Green-Kubo relation $G(t) = V \langle \sigma_{\alpha\beta}(t) \sigma_{\alpha\beta}(0) \rangle / k_B T$ with $\alpha \neq \beta$ the from stress fluctuations in unstrained, equilibrated melts. The classical expression (data not shown) shows poor collapse of data from different strains due to non-linear effects due to entanglements. The Doi-Edwards expression is comparable to the classical theory for early times, but has an improved data collapse at later times. The slip-tube expression leads to a satisfactory data collapse and good agreement with the Green-Kubo results, suggesting that it accurately captures the non-linear effects at large strains.

In Figure 2a we show a comparison of the simulation results for $G(t)$ to the predictions of the Rouse model [3, 34] for unentangled systems. Our results confirm the expectation that the Rouse model quantitatively describes the chain length independent early-time stress relaxation with $G(t) \propto t^{-1/2}$ as well as terminal stress relaxation in systems with chains too short to be entangled. Entanglements start to affect the behavior of sufficiently long chains beyond a material-specific, characteristic time $\tau_e \approx 10^4\tau$. In particular, we clearly observe a

plateau in the stress relaxation for our longest chain systems with $Z = 40$. For the terminal stress relaxation of systems with $Z = \mathcal{O}(10)$ we have reliable data extending about one order of magnitude below the plateau level. This is sufficient to allow for a meaningful comparison to current theories. In particular, we are not restricted to comparing the ability of different theories to fit the data. Rather, we can carry out *absolute, parameter-free* comparisons using the result $N_e = 90 \pm 10$ [24] of the primitive path analysis and the known monomeric (Rouse) friction of the model.

Likhtman and McLeish (LM) [35] assembled the effects of (i) early-time Rouse relaxation, (ii) tension equilibration along the contour of the primitive chains, (iii) reptation, (iv) contour length fluctuations, and (v) constraint release into a closed functional form,

$$G(t) = \frac{\rho k_B T}{N} \left(\frac{4}{5} Z \mu(t) R(t) + \frac{1}{5} \sum_{p=1}^{Z-1} e^{-tp^2/\tau_R} \right) + \frac{\rho k_B T}{N} \sum_{p=Z}^N e^{-2tp^2/\tau_R} \quad (2)$$

where $\mu(t)$ is the single-chain memory function, and $R(t)$ is the tube memory function describing the Rouse-like motion of the tube due to constraint release events. In the absence of the relaxation processes described by the tube model ($\mu(t) = R(t) \equiv 1$), the formula describes a crossover from the early time Rouse relaxation $G(t) \propto t^{-1/2}$ to a plateau $G_N^0 = \frac{4}{5} \frac{\rho k_B T}{N_e}$. The key quantity of the tube model is the single-chain memory function, $\mu(t)$, for the fraction of the primitive chain which has not escaped from its original tube after a time t . Comparisons to the data neglecting constraint release ($R(t) \equiv 1$) are shown in Figs. 2 b, c and e for the original Doi-Edwards model accounting only for reptation, Doi's approximate inclusion of contour length fluctuations [3] with a maximal relaxation time from [35], and the Likhtman-McLeish theory [35] respectively. For the comparisons in Figs. 2d and f we have included the effect of constraint release in the double reptation [36] approximation $R(t) = \mu(t)$, but we note that LM used a more rigorous, self-consistent formalism [37] for coupling constraint release to the single chain relaxation processes.

The overall agreement between our data and the more advanced versions of the tube model is fairly good. Interestingly, the more sophisticated LM theory seem to work less well than the Doi's approximation. Yet, from our rheological data alone, it is hard to clearly identify the relevant relaxation processes. For example, one might (as we believe, erroneously; see below) conclude, that the double reptation approximation strongly overestimates the contribution of constraint release to the stress relaxation (Figs. 2e and f) or that constraint release is inefficient for $Z < 4$ (Figs. 2c and d). Obviously, fitting the data to the various theories would only obscure their shortcomings.

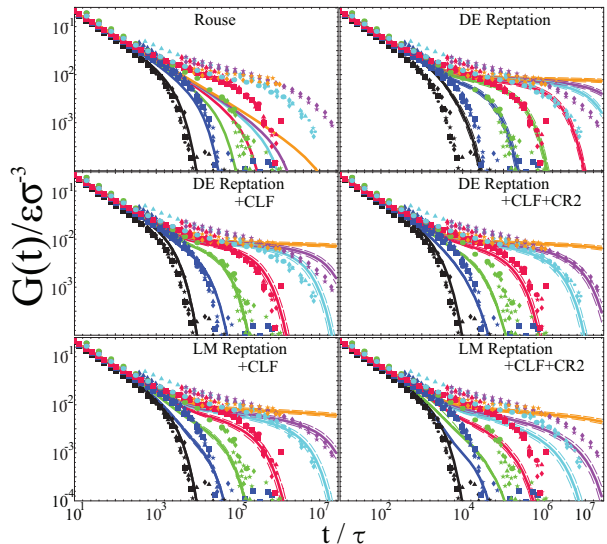


FIG. 2: (color online) Comparison of the measured relaxation moduli to the predictions of various theories. Symbols and colors for the simulation data in Fig. 1c. Theoretical predictions are shown as thick lines using the same color code. Thin lines indicate the uncertainty in the theoretical predictions due to the uncertainty of the PPA entanglement length $N_e = 90 \pm 10$.

To draw definite conclusion on how to improve the theories, we discriminate in the following three possible sources of error in the present theoretical framework: (i) the functional form of Eq. (2), (ii) the treatment of reptation and contour length fluctuations underlying the single-chain memory function $\mu(t)$, and (iii) the treatment of the multi-chain effect of constraint release via the double reptation approximation, $R(t) = \mu(t)$. Under the assumption that the escaped chain sections equilibrate completely, $\mu(t)$ equals the autocorrelation function of the chain end-to-end vectors, which is easily accessible from our equilibrium simulations. In Fig. 3 we show a comparison between the measured relaxation moduli and those predicted from Eq. (2) using the measured $\mu(t)$ and $R(t) = \mu(t)$. The agreement is excellent, supporting the utility of both the Likhtman-McLeish functional form of the shear relaxation modulus and of the double reptation approximation [36]. The shortcomings of the LM description observed here and in the rheological study by Liu *et al.* [7] must thus be related to the central part of their theory, the estimation of the time dependence of the fraction, $\mu(t)$, of surviving tube sections under the combined influence of reptation and contour length fluctuations. This poses an intriguing puzzle, since the inclusion of contour length fluctuations is essential for obtaining a

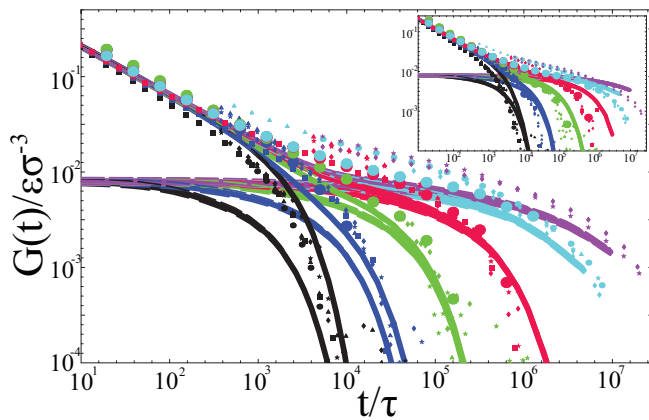


FIG. 3: (color online) Comparison of the measured relaxation moduli to Eq. (3) using an independently measured estimate of the tube memory function, $\mu(t)$, the autocorrelation function of the chain end-to-end vectors. The upper set of curves corresponds to the full theoretical expression, while the lower set of curves only shows the most slowly decay term, $\frac{4}{5}G_e\mu(t)R(t)$. In the figure, we have used the double reptation approximation, $R(t) \equiv \mu(t)$, while the inset shows a comparison to the model without constraint release, $R(t) \equiv 1$. Symbols and colors as in Fig. 2.

coherent description of neutron-spin echo results on the conformational relaxation [10].

To summarize, we have presented an extensive set of simulation results for the equilibrium and relaxation dynamics of entangled model polymer melts. We have shown that the use of the stress-strain relation of the slip-tube model [31] as damping function results in excellent agreement between equilibrium and non-equilibrium measurements of $G(t)$. In particular, we explored $G(t)$ into the plateau regime for chains with $Z = 40$ and into the terminal relaxation regime for $Z \leq 10$ and compared our data to predictions of different versions of the tube model. These comparisons did not involve any free parameters, since the entanglement length was determined independently via a topological analysis [17, 24]. The overall agreement is very good, demonstrating that the primitive path analysis of the microscopic *structure* endows the tube model with predictive power for *dynamical processes*. Moreover, we have shown that with the presently accessible chain lengths and time scales and the simultaneous access to stress and conformational relaxation, computer simulations are now in a position to subject tube models to detailed tests, allowing, for example, to independently validate the quality of the theoretical treatment of single- and multi-chain relaxation processes.

We thank the New Mexico Computing Application Center NMCAC for generous allocation of computer time and A. Likhtman and S.K. Sukumaran for their Green-Kubo data from [27]. C.S. acknowledges financial support from the Danish Natural Sciences Research

Council through a Steno Research Assistant Professor fellowship. J.H. is supported by the EC through the Marie Curie EST *Eurosim* Project No. MEST-CT-2005-020491. R.E. acknowledges a chair of excellence grant from the Agence Nationale de Recherche (France). Sandia is a multiprogram laboratory operated by Sandia Corporation, a Lockheed Martin Company, for the U.S. Department of Energy under Contract No. DE-AC04-94AL85000.

* Electronic address: science@zqex.dk

- [1] J. D. Ferry, *Viscoelastic Properties of Polymers* (Wiley, New York, 1980).
- [2] R. B. Bird, R. C. Armstrong, and O. Hassager, *Dynamics of Polymeric Liquids*, vol. 1 (Wiley, New York, 1977).
- [3] M. Doi and S. F. Edwards, *The Theory of Polymer Dynamics* (Clarendon, Oxford, 1986).
- [4] T. C. B. McLeish, *Adv. Phys.* **5**, 1379 (2002).
- [5] S. F. Edwards, *Proc. Phys. Soc.* **92**, 9 (1967).
- [6] P. G. de Gennes, *J. Chem. Phys.* **55**, 572 (1971).
- [7] C.-Y. Liu, R. Keunings, and C. Bailly, *Phys. Rev. Lett.* **97**, 246001 (2006).
- [8] H. Watanabe, *Prog. Polym. Sci.* **24**, 1253 (1999).
- [9] B. Ewen and D. Richter, *Adv. Pol. Sci.* **134**, 3 (1997).
- [10] A. Wischniewski, M. Monkenbusch, L. Willner, D. Richter, A. Likhtman, T. McLeish, and B. Farago, *Phys. Rev. Lett.* **88**, 58301 (2002).
- [11] P. T. Callaghan and E. T. Samulski, *Macromolecules* **30**, 113 (1997).
- [12] K. Saalwchter, *Progr. NMR Spectrosc.* **51**, 1 (2007).
- [13] K. Kremer and G. S. Grest, *J. Chem. Phys.* **92**, 5057 (1990).
- [14] M. Kröger and S. Hess, *Phys. Rev. Lett.* **85**, 1128 (2000).
- [15] P. V. K. Pant and D. N. Theodorou, *Macromolecules* **28**, 7224 (1995).
- [16] R. Auhl, R. Everaers, G. S. Grest, K. Kremer, and S. J. Plimpton, *J. Chem. Phys.* **119**, 12718 (2003).
- [17] R. Everaers, S. K. Sukumaran, G. S. Grest, C. Svaneborg, A. Sivasubramanian, and K. Kremer, *Science* **303**, 823 (2004).
- [18] S. K. Sukumaran, G. S. Grest, K. Kremer, and R. Everaers, *J. Polym. Sci, Part B: Polym. Phys.* **43**, 917 (2005).
- [19] M. Kröger, *Comp. Phys. Comm.* **168**, 209 (2005).
- [20] S. Shanbhag and R. G. Larson, *Phys. Rev. Lett.* **94**, 076001 (2005).
- [21] Q. Zhou and R. G. Larson, *Macromolecules* **38**, 5761 (2005).
- [22] C. Tzoumanekas and D. N. Theodorou, *Macromolecules* **39**, 4592 (2006).
- [23] N. Uchida, G. S. Grest, and R. Everaers, *J. Chem. Phys.* **128**, 044902 (2008).
- [24] R. S. Hoy, K. Foteinopoulou, and M. Kröger, *Phys. Rev. E* **80**, 031803 (2009).
- [25] S. Plimpton, *J. Comp. Phys.* **117**, 1 (1995).
- [26] R. Everaers and K. Kremer, *Macromolecules* **28**, 7291 (1995).
- [27] A. E. Likhtman, S. K. Sukumaran, and J. Ramirez, *Macromolecules* **40**, 6748 (2007).
- [28] G. Marrucci and B. de Cindio, *Rheol. Acta* **19**, 68 (1980).

- [29] F. Greco, Phys. Rev. Lett. **88**, 108301 (2002).
- [30] O. Urakawa, M. Takahashi, T. Masuda, and N. G. Ebrahimi, Macromolecules **28**, 7196 (1995).
- [31] M. Rubinstein and S. Panyukov, Macromolecules **35**, 6670 (2002).
- [32] C. Svaneborg, R. Everaers, G. S. Grest, and J. G. Curro, Macromolecules **41**, 4920 (2008).
- [33] [1] Eqs.(7.137)-(7.141).
- [34] P. E. Rouse, J. Chem. Phys. **21**, 1273 (1953).
- [35] A. Likhtman and T. McLeish, Macromolecules **35**, 6332 (2002).
- [36] J. des Cloizeaux, Europhys. Lett. **5**, 437 (1988).
- [37] M. Rubinstein and R. H. Colby, J. Chem. Phys. **89**, 5291 (1988).